Supplemental Data

Supplementary Table 1. The sources of commercial antibodies and the concentrations of the antibodies used for immunofluorescence (IF), immunoblotting (IB), or immunoprecipitation (IP)

Antibody	Animal	Vendor	Catalog number	RRID	Dilution	Application
Insulin	Guinea pig serum	H. Kobayashi (Gunma University)			1/500	IF
Granuphilin	Rabbit polyclonal	Homemade (Ref. 19)	αGrp-N		IB 1/1000 IF 1/100	IB, IF
Melanophilin	Goat polyclonal	Everest Biotech, Oxfordshire, UK	EB05444	AB_2297905	1/1000	IB
Melanophilin	Rabbit polyclonal	Abcam, Cambridge, UK	Ab137078	AB_2732921	1/1000	IB
HA (hemagglutinin)	Rabbit polyclonal	MBL, Nagoya, Japan	561	AB_591839	1/1000	IB
HA (3F10)	Rat monoclonal	Roche Diagnostics GmbH, Mannheim, Germany	11867423001	AB_390918	1/100	IF
GAPDH	Mouse monoclonal	MBL, Nagoya, Japan	M171-3	AB_10597731	1/1000	IB
FLAG	Rabbit polyclonal	Sigma-Aldrich, St.Louis, MO	F7425	AB_439687	IB 1/5000; IF 1/500	IB, IF
β-actin	Mouse monoclonal	Sigma-Aldrich, St.Louis, MO	A5316	AB_476743	1/10000	IB
α-tubulin	Mouse monoclonal	Sigma-Aldrich, St.Louis, MO	T5168	AB_477579	1/10000	IB
Munc18-3	Rabbit polyclonal	Sigma-Aldrich, St.Louis, MO	M7695	AB_1080121	1/1000	IB
Syntaxin-1	Mouse monoclonal	Sigma-Aldrich, St.Louis, MO	S0664	AB_477483	1/1000	IB
Syntaxin-2	Rabbit polyclonal	Synaptic Systems, Goettingen, Germany	110 123	AB_887849	1/1000	IB
Syntaxin-3	Rabbit polyclonal	Synaptic Systems, Goettingen, Germany	110 033	AB_887851	1/1000	IB
Syntaxin-4	Rabbit polyclonal	Synaptic Systems, Goettingen, Germany	110 043	AB_10693907	IF 1/200; IP 2 μg /sample	IF, IP
Syntaxin-4	Rabbit polyclonal	Merck KGaA, Darmstadt, Germany	AB5330	AB_91042	1/1000	IB

Myosin-Va	Rabbit polyclonal	Cell Signaling Technology, Danvers, MA	3402	AB_2148475	1/1000	IB
Myosin-Va	Rabbit polyclonal	Sigma-Aldrich, St.Louis, MO	M4812	AB_260545	1/100	IF
VAMP2	Rabbit polyclonal	Calbiochem, San Diego, CA	627724	AB_212589	1/500	IB
Munc18-2	Rabbit polyclonal	LifeSpan BioSciences, Inc., Seattle, WA	LS-B2356	AB_2271157	1/1000	IB
Rab27a	Mouse monoclonal	BD BioScience, San Jose, CA	558532	AB_647327	IB 1/1000; IF 1/100	IB, IF
SNAP25	Mouse monoclonal	BD BioScience, San Jose, CA	610366	AB_397752	1/1000	IB
Munc18-1	Mouse monoclonal	BD BioScience, San Jose, CA	610336	AB_397726	1/10000	IB
Anti-RFP	Rabbit polyclonal	MBL, Nagoya, Japan	PM005	AB_591279	1/1000	IB
EB1	Mouse monoclonal	BD BioScience, San Jose, CA	610534	AB_397891	1/1000	IB
Anti-MBP		New England Biolabs, Ipswich, MA	E8032	AB_1559730	1/10000	IB
Anti-GST		Upstate Biotechnology, New York, NY	05-311	AB_309675	1/5000	IB
Rhodamine-conjugated phalloidin		Thermo Fisher Scientific, Waltham, MA	R415	AB_2572408	1/100	IF
Anti-HA Affinity Matrix	Rat monoclonal	Roche Diagnostics GmbH, Mannheim, Germany	11815016001	AB_390914	20 µl /sample	IP
Anti-FLAG M2 Affinity Gel	Rabbit polyclonal	Sigma-Aldrich, St.Louis, MO	A2220	AB_10063035	30 µl /sample	IP
Protein G Sepharose 4 Fast Flow		GE Healthcare Biosciences, Piscataway, NJ	GE17-0618-01		40 µl /sample	IP
StrepTactin Sepharose High Performance		GE Healthcare Biosciences, Piscataway, NJ	GE28-9355-99		30 µl /sample	IP
Amylose Resin		New England Biolabs, Ipswich, MA	E8021		20 µl /sample	IP

Supplemental Table 2. Primer for cloning, mutagenesis, and quantitative PCR

Target	Primer	Sequence
Melanophilin full length	Forward	GGGGAATTCATGGGGAAAAGGTTGGACCT
	Reverse	GGGCTCGAGTTAGGGCTGCTGGGCCATC
Melanophilin fragment N (1-400)	Forward	GGGGAATTCATGGGGAAAAGGTTGGACCT
	Reverse	GGGCTCGAGTTAGGTGCTGGAACCACTGATG
Melanophilin fragment 116-400	Forward	GGGGAATTCATGGGTTCTCTGGAGTGGTACTA
Melanophilin fragment 126-400	Forward	GGGGAATTCATGAGGGCTCGCTTCAAGCGTT
Melanophilin fragment C (147-590)	Forward	GGGGAATTCATGGGTGGAGGTGGATCTGAGC
	Reverse	GGGCTCGAGTTAGGGCTGCTGGGCCATC
Melanophilin fragment 1-100	Forward	GGGCTCGAGCTATGGGGAAAAGGTTGGACCT
	Reverse	GGGGAATTCTTACTGCTCTTCTGGGTGGGC
Melanophilin fragment 1-110	Reverse	GGGGAATTCTTAGGCCAGGTGGCAGGGGTC
Melanophilin fragment 1-120	Reverse	GGGGAATTCTTACCACTCCAGAGAACCGAT
Melanophilin fragment 1-130	Reverse	GGGGAATTCTTACTTGAAGCGAGCCCTCAC
Melanophilin fragment 1-146	Reverse	GGGGAATTCTTACTGCAGCCGCCCACAGAG
Melanophilin mutation E14A	Forward	ACAGACGAGGCGGCTGAGCAC
	Reverse	GTGCTCAGCCGCCTCGTCTGT
Melanophilin mutation D378A/E380A/E381A/E382A	Forward	CCCAGTGCTGCCACAGCGGCGGCGACACTCAGG
	Reverse	CCTGAGTGTCGCCGCCGCTGTGGCAGCACTGGG
Melanophilin mutation A467P	Forward	GTTCAGCAGCCTGAGAGTGAG
	Reverse	CTCACTCTCAGGCTGCTGAAC
Melanophilin mutation Y122A	Forward	GAGTGGTACGCCCAGCACGTGAGG
	Reverse	CCTCACGTGCTGGGCGTACCACTC
Melanophilin mutation H124AK130A	Forward	CAGGCCGTGAGGGCTCGCTTCGCGCGTTTC
	Reverse	ACTCCCGAAACGCGCGAAGCGAGCCCTCAC

Melanophilin full length (for EGFP or mCherry tag)	Forward	GGGCTCGAGCTATGGGGAAAAGGTTGGACCT
	Reverse	GGGGAATTCTTAGGGCTGCTGGGCCATC
Syntaxin-4 full length	Forward	GGGGAATTCATGCGCGACAGGACCCAC
	Reverse	GGGCTCGAGTTATCCAACGGTTATGGTGATG
Syntaxin-4 N-Habc fragment (1-193)	Forward	GGGGAATTCATGCGCGACAGGACCCAC
	Reverse	GGGCTCGAGTTACGTGTCCTTCAGGATATTAGA
Syntaxin-4 H3 fragment (194-273)	Forward	GGGGAATTCATGCAGGTGACTCGGCAGGCC
	Reverse	GGGCTCGAGTTACGTGTCCTTCAGGATATTAGA
Syntaxin-4 mutation L173A/E174A	Forward	GAGGAGGCGGCACAGATG
	Reverse	CATCTGTGCCGCCTCCTC
Human melanophilin quantitative PCR	Forward	GATGGAGAACCTGGCTCAGA
	Reverse	GGAGAGGAGGCGCTTTTT
GAPDH quantitative PCR	Forward	AGGGCTGCTTTTAACTCTGGT
	Reverse	CCCCACTTGATTTTGGAGGGA

Supplementary Figures

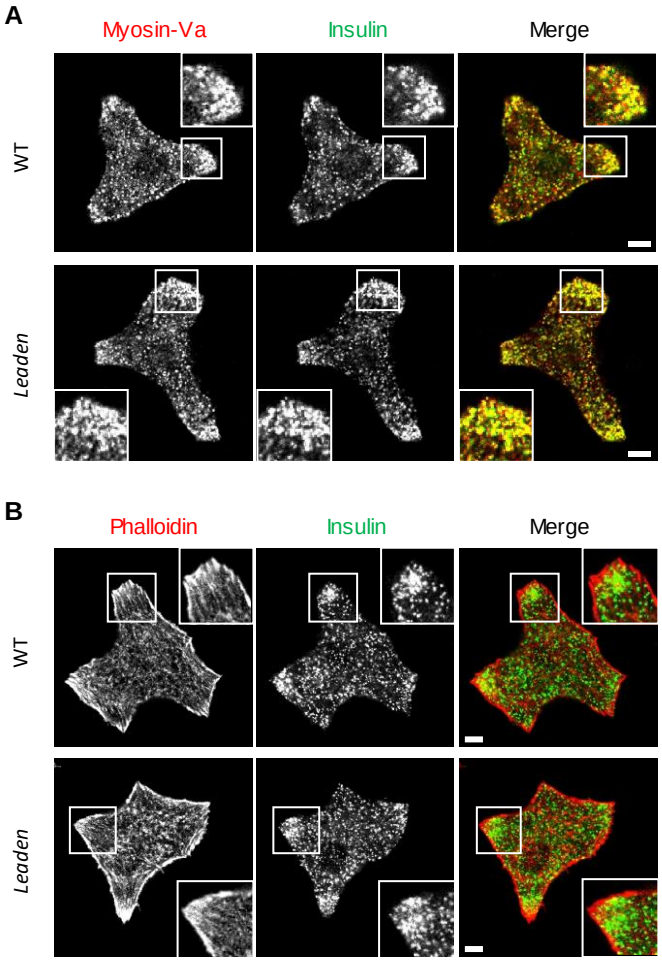

Supplementary Figure 1. Insulin granules accumulates in the actin-rich cell periphery independent of the presence or absence of melanophilin in β cells
A monolayer of pancreatic islet cells isolated from wild-type or *leaden* mice was fixed and double-stained with anti-insulin antibody and either anti-myosin-Va antibody (upper) or rhodamine-conjugated phalloidin that binds filamentous actin (lower). Insets represent higher magnification micrographs of cells within the region outlined by frames. Bars, 5 μm.

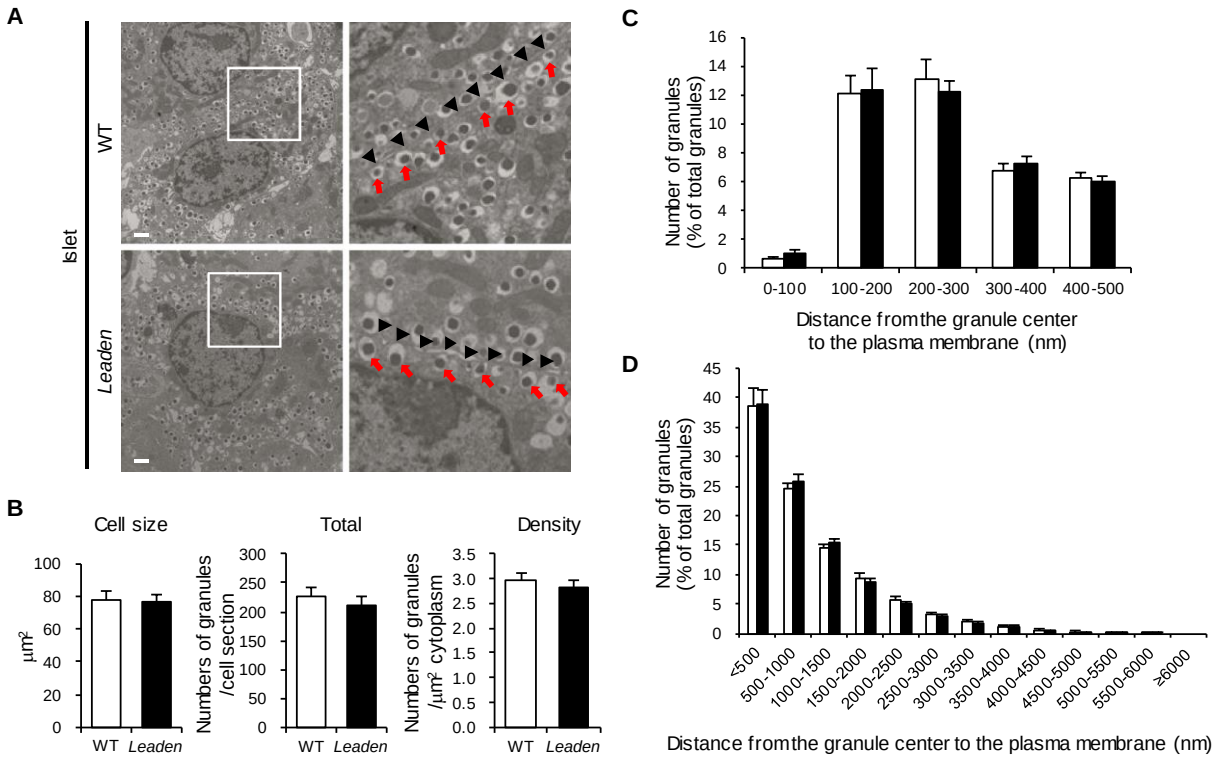

Supplementary Figure 2. The distribution of insulin granules is not altered in *leaden* β cells
Islets isolated from 24- to 28-week-old, wild-type (open bars) and *leaden* mice (closed bars) were fixed by immersion with 2% paraformaldehyde, 2% glutaraldehyde, 0.2% picric acid in 0.1 M cacodylate buffer, pH 7.4, for 1.5 h at room temperature and embedded into 1% agarose. They were then postfixed, embedded in plastic resin, and sectioned. The ultrathin sections (80 nm) were observed by electron microscopy. (A) Micrographs were randomly taken at 5000 and 8000 magnifications from 21 individual cells from three mice for each genotype. Squares in left panels are shown at a higher magnification in right panels. Black arrowheads indicate the position of the plasma membrane, whereas red arrows indicate granules directly attached to the plasma membrane. Bar, 1 µm. (B) Cell size (left), total number of granules (middle), and average granule density (right). (C, D) Granules whose centers located within 500 nm from the plasma membrane (C) or total granules (D) were categorized according to the distance from the granule center to the plasma membrane. The statistical significance of differences between means was assessed by Student's *t*-test.

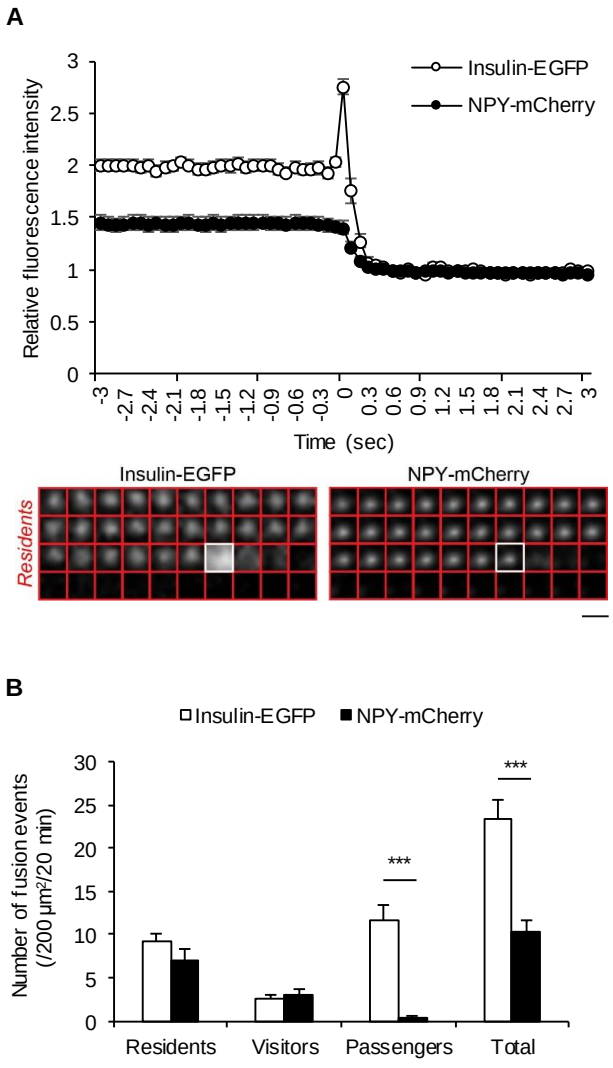

Supplementary Figure 3. Granules visualized by pH-insensitive NPY-mCherry lack a fluorescence intensity peak and exhibit no *passenger* type of exocytosis

(A) A monolayer of pancreatic islet cells isolated from wild-type mice was infected with adenovirus encoding Insulin-EGFP or NPY-mCherry, and was stimulated by 25 mM glucose for 20 min under TIRF microscopy. The fluorescence intensity profiles during the *resident* type of exocytosis (upper) are shown as the mean ± SEM for granules labeled by Insulin-EGFP (n = 20 from 10 cells) and those labeled by NPY-mCherry (n = 22 from 8 cells). Kymographs are the sequential TIRF microscopic images acquired every 103 ms during the *resident* type of exocytosis (lower). Note that granules labeled by NPY-mCherry lack a fluorescence intensity peak during fusion, in contrast to those labeled by Insulin-EGFP. Bar, 1 μm. (B) Numbers of fusion events during 25 mM glucose stimulation for 20 min in wild-type mouse islet cells expressing NPY-mCherry (closed bars; n = 10 cells) were compared with those in cells expressing Insulin-EGFP shown in Fig. 2C (open bars; n = 32 cells). Note that there is almost no *passenger* type of exocytosis in cells expressing NPY-mCherry due to the lack of a flash phenomenon accompanied by a fusion event. $^{***}P < 0.001$; Student's t-test.

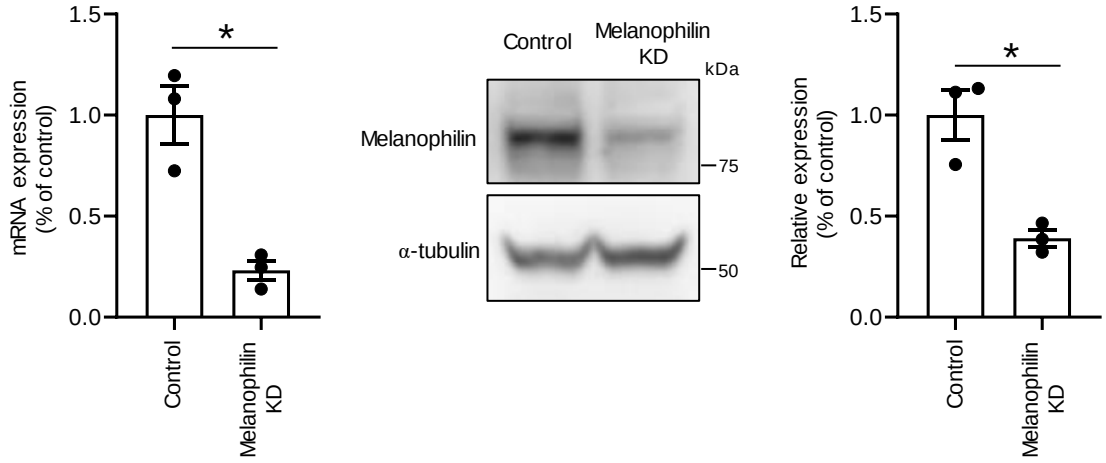

Supplementary Figure 4. Downregulation of melanophilin in human islet cells
Melanophilin was knockdown (KD) in human islet cells by siRNA followed by shRNA as described in Research Designs and Methods. The cells were analyzed for melanophilin expression 48 h after the shRNA adenovirus infection. Downregulation was verified by quantitative PCR (left; $n = 3$) and immunoblotting (middle). Protein bands were quantified by densitometric analyses from three independent preparations (right). $^{*}P < 0.05$; Student's *t*-test.

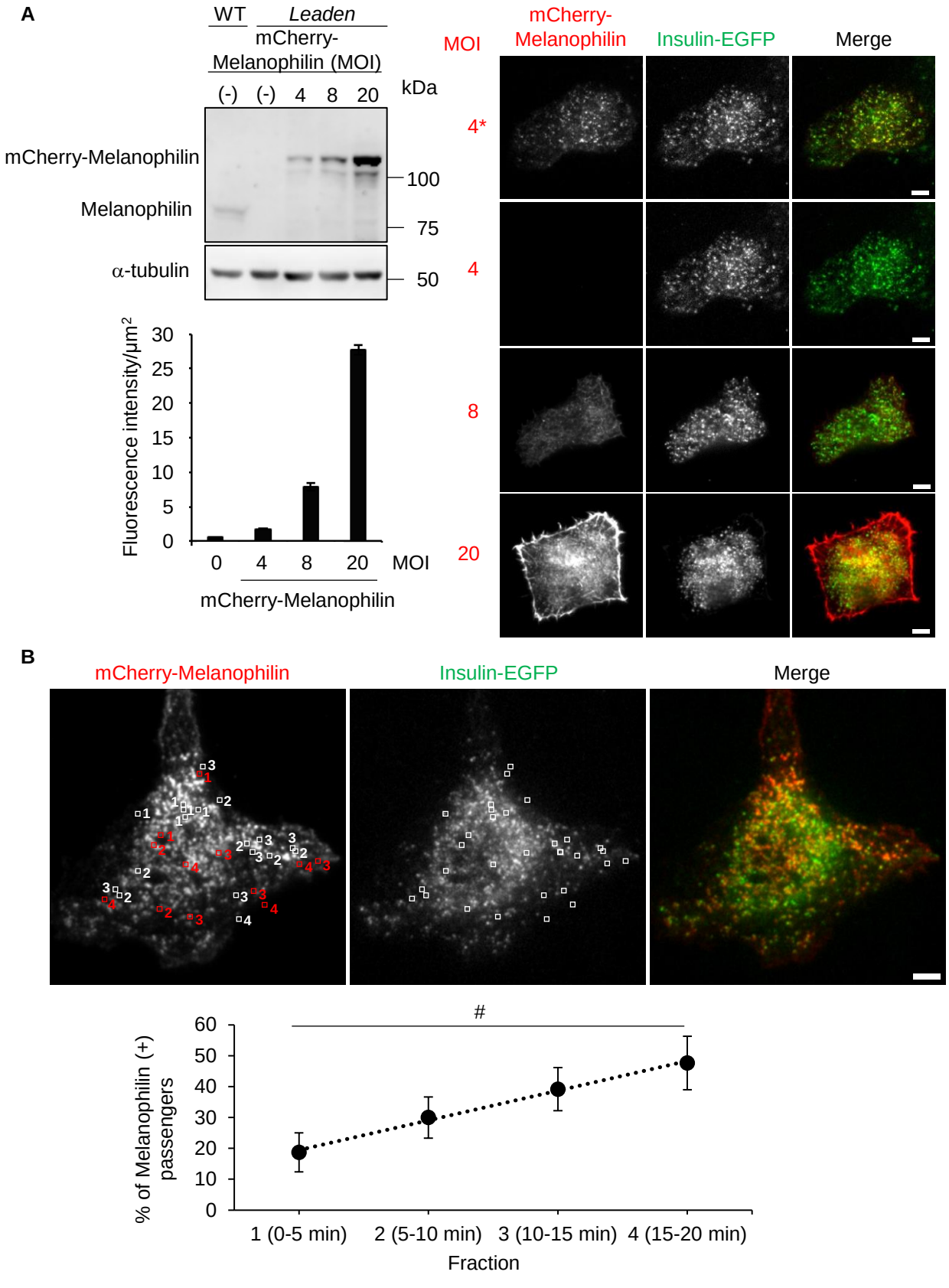
A
WT
Leaden
mCherry-Melanophilin (MOI)
(-) (-) 4 8 20
kDa
mCherry-Melanophilin
Melanophilin
α-tubulin
100
75
50
Fluorescence intensity/μm²
30
25
20
15
10
5
0
0 4 8 20 MOI
mCherry-Melanophilin
MOI
mCherry-Melanophilin
Insulin-EGFP
Merge
4*
4
8
20
B
mCherry-Melanophilin
Insulin-EGFP
Merge
#
% of Melanophilin (+) passengers
60
50
40
30
20
10
0
1 (0-5 min)
2 (5-10 min)
3 (10-15 min)
4 (15-20 min)
Fraction

Supplementary Figure 5. Localization of mCherry-melanophilin expressed in *leaden* islet cells

(A) A monolayer of *leaden* islet cells was infected with adenovirus encoding Insulin-EGFP at MOI 10 and that encoding mCherry-melanophilin at MOI 4, 8, or 20. The expression levels were examined by immunoblotting with anti-melanophilin and anti-α-tubulin antibodies (upper left), which indicated that the expression level of mCherry-melanophilin at MOI 4 was similar to that of endogenous melanophilin. The fluorescence intensity (lower left; n = 84, 28, 24, and 32 cells from 3 mice for MOI = 0, 4, 8, or and 20, respectively) and the localization (right) of mCherry melanophilin were examined by TIRF microscopy. Because the signal of mCherry-melanophilin expressed at MOI 4 was weak (the second raw), it was enhanced at 15 times (close to the maximum; 4* in the first raw). Although mCherry-melanophilin localized on granules when expressed at the endogenous level (MOI 4), it exhibited a filamentous distribution, likely along F-actin, when expressed only at two times of the endogenous level (MOI 8). (B) A monolayer of *leaden* islet cells was infected with adenovirus encoding Insulin-EGFP and that encoding mCherry-melanophilin at MOI 4 as described above (n = 22 cells from 7 mice). Cells were stimulated by 25 mM glucose for 20 min, and fusion events were recorded under TIRF microscopy as described in Fig. 2. After the experiments, cells were immediately fixed with 3% paraformaldehyde and were immunostained with anti-RFP antibody to detect mCherry melanophilin. Boxes in the Insulin-EGFP image indicate the positions where the *passenger* exocytosis occurs, although they lack EGFP signals in a post-fusion still image. Red boxes at corresponding positions in the mCherry-melanophilin image indicate the presence of melanophilin, whereas white ones indicate its absence. *Passengers* are categorized into 4 bins and labeled as 1-4 according to the time of fusion events after glucose stimulation. The graph shows the percentage of melanophilin-positive *passengers* in each bin. Granules fused at early time points (1: 0-5 min and 2: 5-10 min) tend to lack melanophilin compared with those fused at later time points (3: 10-15 min and 4: 15-20 min), likely due to occurrence of post-fusion events such as endocytosis during a period from time of fusion till cell fixation at 20 min. $^{\#}P < 0.05$; one-way ANOVA. Bars, 5 μm.

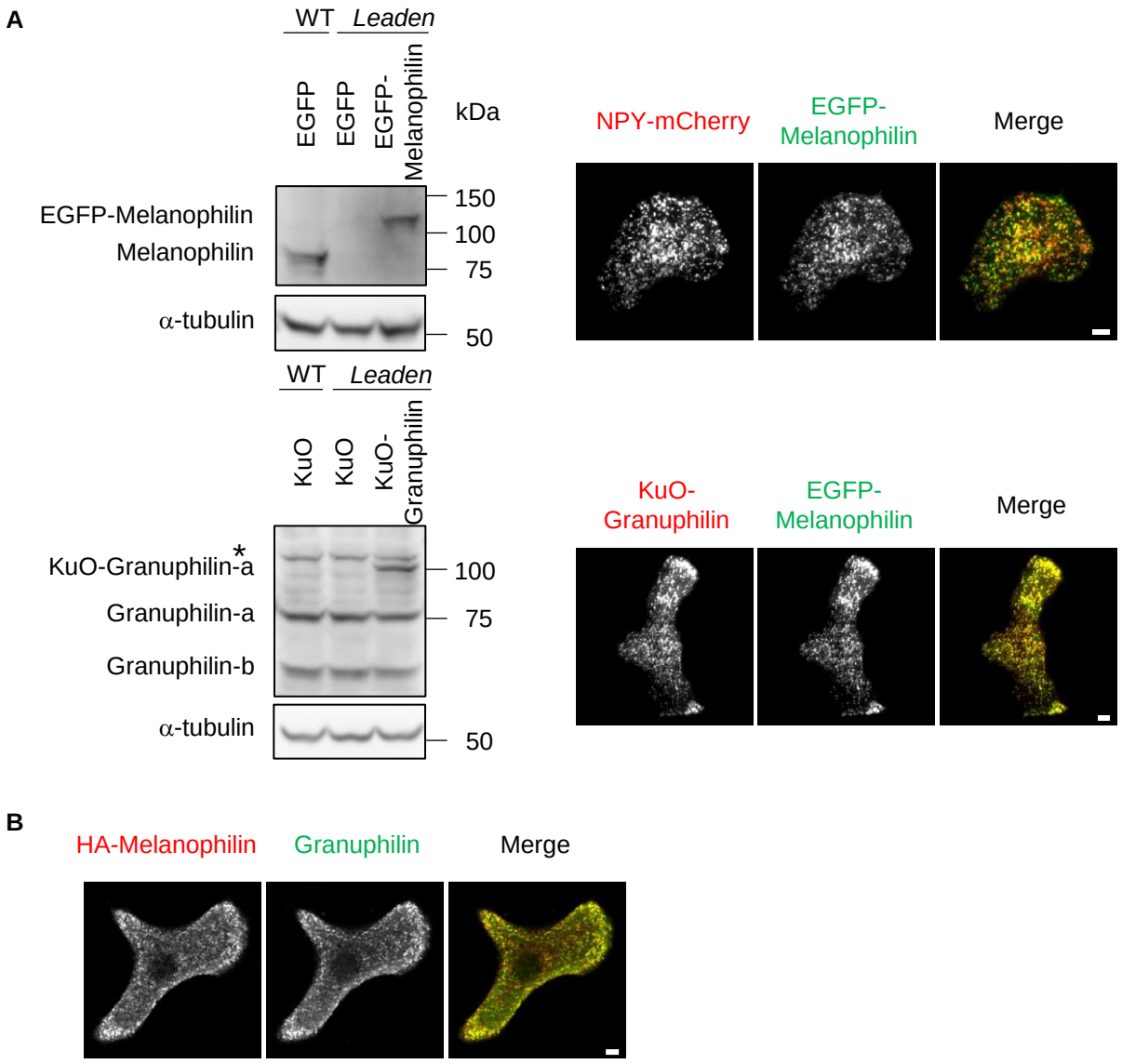

Supplementary Figure 6. Colocalization of melanophilin and granuphilin on the same granules in *leaden* islet cells

(A) A monolayer of wild-type or *leaden* islet cells was infected with adenovirus encoding EGFP-melanophilin or EGFP only (upper left), or that encoding KuO-granuphilin or KuO only (lower left). Immunoblotting revealed that both EGFP-melanophilin and KuO-granuphilin are expressed in *leaden* cells at endogenous protein levels found in wild-type cells. The band highlighted with an asterisk is a nonspecific protein. At these expression levels, 90 and 97% of EGFP-melanophilin colocalize with NPY-mCherry (upper right) and KuO-granuphilin (lower right, respectively, under TIRF microscopy (n = 27-28 islet cells from 4 *leaden* mice). (B) A monolayer of *leaden* islet cells expressing HA-melanophilin at an endogenous level was immunostained with anti-HA and anti-granuphilin antibodies. Confocal microscopy revealed that 95% of HA-malanophilin colocalizes with endogenous granuphilin (n = 18 cells from 3 mice). Bars, 5 μm.

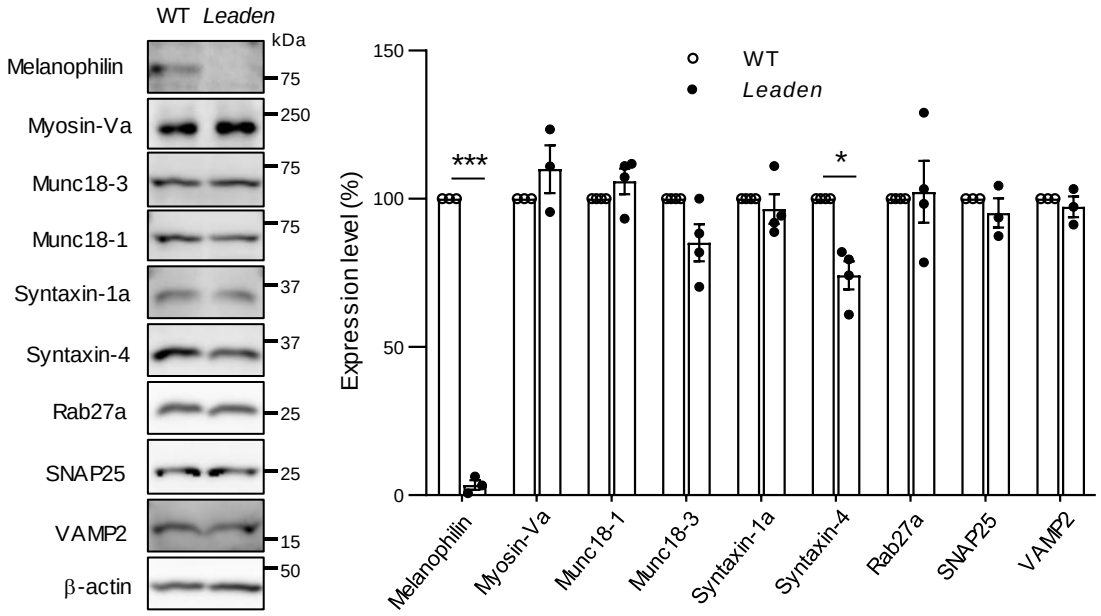

Supplementary Figure 7. The expression level of syntaxin-4 is decreased in *leaden* islets
Islets extracts (30 μg) from wild-type and *leaden* mice were immunoblotted with antibodies toward the indicated proteins (left). Protein expression levels (wild type: open dots; *leaden*: closed dots) were quantified by densitometric analyses from 3-4 independent preparations (right). $^{*}P < 0.05$, $^{***}P < 0.001$; Student's *t*-test.

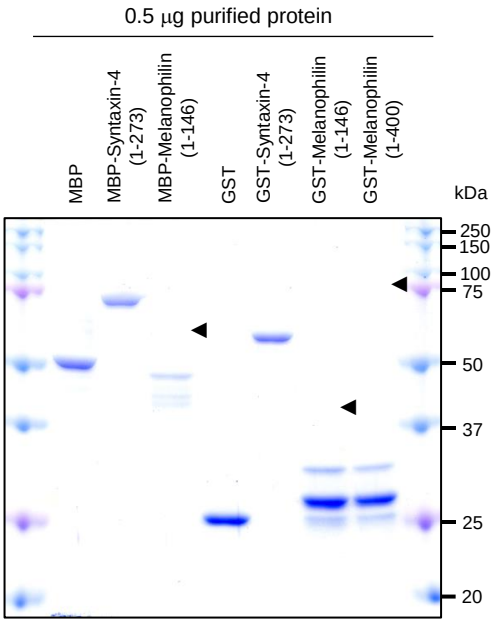

Supplementary Figure 8. Affinity-purified, syntaxin-4 and melanophilin proteins expressed in bacteria

Indicated amino acid portions of syntaxin-4 and melanophilin were expressed in *E. coli*, BL21 (DE3). Proteins were purified using amylose-agarose or glutathione-Sepharose 4B, and were subjected to SDS-PAGE and Coomassie Brilliant Blue staining. Although syntaxin-4 with either MBP or GST tag was efficiently expressed and purified, two different syntaxin-4-binding domains of melanophilin was not. Therefore, protein interaction experiments in Fig. 4G were performed between syntaxin-4 (0.5 μg) and 40-fold excess of melanophilin containing its degradation products (20 μg). Arrowheads indicate the expected positions of each melanophilin protein with corresponding molecular mass.

Video Legend

Video 1. Granules labeled by pH-insensitive NPY-mCherry lack a flash during fusion

A monolayer of pancreatic islet cells isolated from wild-type mice was infected with adenovirus encoding Insulin-EGFP (left) or NPY-mCherry (right), and was stimulated by 60 mM KCl for 1 min under TIRF microscopy. Images were sampled every 103 ms, and videos were forwarded at a 3-times speed. Note that pH-insensitive mCherry-labeled granules do not exhibit a flash phenomenon during fusion, in which the pH-sensitive EGFP-fused, cargo protein lights-up with release and immediately disappears with diffusion. Bar, 10 μm.

Video 2. An example of the *resident* type of exocytosis in human pancreatic β cells

Human pancreatic β cells expressing Insulin-EGFP were stimulated with 25 mM glucose under TIRFM. The images taken every 103 ms for 20 s are shown in a twice speed-forwarded video. Bar, 1 μm.

Video 3. An example of the *passenger* type of exocytosis in human pancreatic β cells

Human pancreatic β cells expressing Insulin-EGFP were stimulated with 25 mM glucose under TIRFM. The images taken every 103 ms for 20 s are shown in a twice speed-forwarded video. Bar, 1 μm.